

~~227~~ 765

SAND78-1147  
Unlimited Release  
UC-70

## Preliminary Thermal Expansion Screening Data for Tuffs

Allen R. Lappin

Prepared by Sandia Laboratories, Albuquerque, New Mexico 87165  
and Berkeley, California 94701 for the California State Department  
of Energy and Resources, Contract DE-AC02-760901789  
Printed March 1980



**Sandia National Laboratories**

8007300222

Issued by Sandia Laboratories, operated for the United States  
Department of Energy by Sandia Corporation.

---

**NOTICE**

This report was prepared as an account of work sponsored by  
the United States Government. Neither the United States nor  
the Department of Energy, nor any of their employees, nor  
any of their contractors, subcontractors, or their employees,  
makes any warranty, express or implied, or assumes any legal  
liability or responsibility for the accuracy, completeness or  
usefulness of any information, apparatus, product or process  
disclosed, or represents that its use would not infringe  
privately owned rights.

Printed in the United States of America

Available from  
National Technical Information Service  
U. S. Department of Commerce  
5285 Port Royal Road  
Springfield, VA 22161  
Price: Printed Copy \$4.50 ; Microfiche \$3.00

SAND78-1147  
Unlimited Release  
Printed March 1980

Distribution  
Category UC-70

PRELIMINARY THERMAL EXPANSION SCREENING DATA FOR TUFFS

Allen R. Lappin  
Geological Projects Division 4537  
Sandia Laboratories  
Albuquerque, New Mexico 87185

ABSTRACT

A major variable in evaluating the potential of silicic tuffs for use in geologic disposal of heat-producing nuclear wastes is thermal expansion. Results of ambient-pressure linear expansion measurements on a group of tuffs that vary greatly in porosity and mineralogy are presented here. Thermal expansion of devitrified welded tuffs is generally linear with increasing temperature and independent of both porosity and heating rate. Mineralogic factors affecting behavior of these tuffs are limited to the presence or absence of cristobalite and altered biotite. The presence of cristobalite results in markedly nonlinear expansion above 200°C. If biotite in biotite-bearing rocks alters even slightly to expandable clays, the behavior of these tuffs near the boiling point of water can be dominated by contraction of the expandable phase. Expansion of both high- and low-porosity tuffs containing hydrated silicic glass and/or expandable clays is complex. The behavior of these rocks appears to be completely dominated by dehydration of hydrous phases and, hence, should be critically dependent on fluid pressure. Valid extrapolation of the ambient-pressure results presented here to depths of interest for construction of a nuclear-waste repository will depend on a good understanding of the interaction of dehydration rates and fluid pressures, and of the effects of both micro- and macrofractures on the response of tuff masses.

## CONTENTS

	<u>Page</u>
Introduction	7
Measurement Description	9
Data Collection Procedure	9
Precision and Accuracy of Measurements	11
Results	14
Expansion Behavior of Devitrified Welded Tuffs	14
Expansion Behavior of Vitric Welded Tuffs and Obsidians	21
Expansion Behavior of Nonwelded Tuffs	25
Conclusions and Discussion	29
References	33
APPENDIX -- Stratigraphic Positions and Sample Locations of Analyzed Samples	35

## ILLUSTRATIONS

### Figure

1	Generalized Map of DOE Nevada Test Site Showing Sample Locations	8
2	Relative Linear Thermal Expansion of Eight Devitrified Welded Tuffs to 500°C	15
3	Relative Linear Thermal Expansion of Samples Ue25A#1-186 and Ue25A#1-2494, Both Devitrified Welded Tuffs	18

ILLUSTRATIONS (cont)

<u>Figure</u>		<u>Page</u>
4	Relative Linear Thermal Expansion of Two Obsidians and Sample Ue25A#1-1290.	24
5	Relative Linear Thermal Expansion of Six Nonwelded Tuffs to 500°C	26
6	Heating-Rate Dependence of Relative Linear Thermal Expansion, Sample GTEv6#1-181	28
7	Linear Expansion Coefficient to 200°C vs Final Porosity of Analyzed Tuffs and Obsidians	31

TABLES

<u>Table</u>		
1	Ambient-Pressure Linear Thermal Expansion Coefficients of Fused Silica as a Function of Temperature	11
2	Linear Thermal Expansion Coefficients of Devitrified Welded Tuffs	16
3	Available Bulk Properties Data	17
4	Linear Thermal Expansion of Devitrified Welded Tuff GTEv6#3-115	21
5	Linear Thermal Expansion Coefficients of Nonwelded Tuffs	27
6	Thermal, Thermogravimetric, and Structural Data for the Most Common Zeolites in Silicic Tuffs	30

## PRELIMINARY EXPANSION SCREENING DATA FOR TUFFS

### Introduction

The Nevada Operations Office (NVO) of the US Department of Energy (DOE) is studying the feasibility of nuclear-waste disposal in silicic tuffs. General material properties data have been collected as part of this study aimed at a preliminary assessment of modeling needs. This report discusses data collected to date on the ambient-pressure thermal expansion of tuffs.

Silicic tuffs, which are fragmental deposits resulting from silicic volcanism, vary greatly in porosity, water content, and both primary and secondary mineralogy. Tuff porosity may range from near 0% to greater than 50%<sup>1</sup> with corresponding water contents. Tuffs differ widely in contents of silicic glass, primary phenocrysts, devitrification products (silica polymorphs plus feldspars and metal oxides), and secondary or authigenic minerals (especially silica polymorphs, feldspars, zeolites, and clays).<sup>2-4</sup>

For reliable thermomechanical modeling of waste disposal in tuffs, it will be necessary to understand within well-defined limits the sensitivity of thermal expansion of a tuff mass to at least the following variables: mineralogy, porosity, temperature, pressure, and time (heating rate). As a first step toward this goal, the objectives of this report are to

1. Report ambient-pressure screening data collected on coherent samples from a broad range of tuffs
2. Make a preliminary assessment of the sensitivity of expansion to porosity and mineralogy

3. Report initial measurements of the rate-dependent expansion of welded and nonwelded tuffs
4. Indicate special areas of interest or concern for examination and evaluation in future studies.

For this report, the ambient-pressure thermal expansion of core samples of 24 different tuffs and 2 obsidians was measured--a total of more than 100 separate runs. Tuffs were taken from localities on the DOE Nevada Test Site (NTS) as shown in Figure 1:

1. Hole Ue25A#1 on the flanks of Yucca Mountain at the western edge of NTS
2. Well J-13 near the western edge of Jackass Flats
3. From within the G-tunnel complex beneath Rainier Mesa.

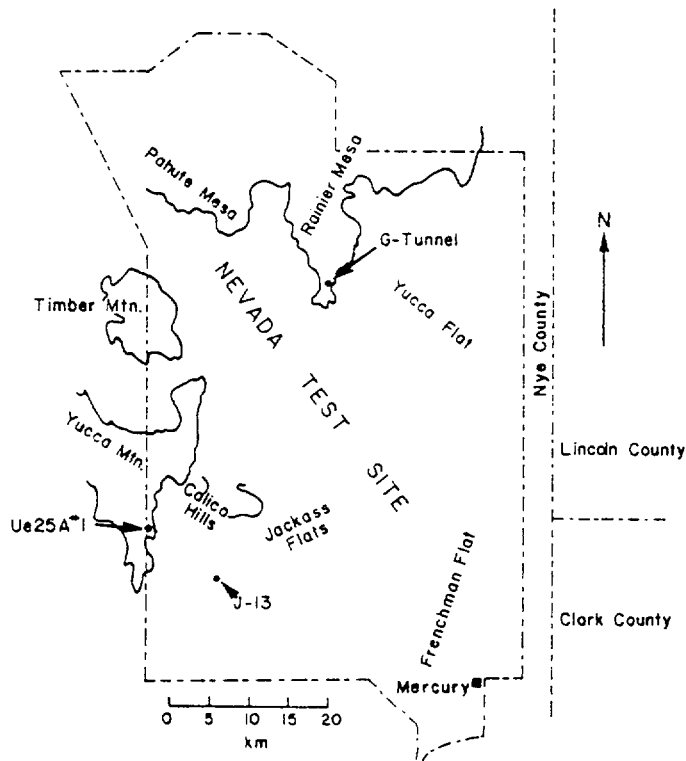


Figure 1. Generalized Map of DOE Nevada Test Site Showing Sample Locations

Sample locations and stratigraphic positions of all analyzed tuffs are given in the Appendix. One obsidian is from the Jemez Mountains of New Mexico and the other from an unknown locality.

## Measurement Description

### Data Collection Procedure

Measurements of linear thermal-expansion coefficients included in this report were made at ambient pressure on a Theta, Inc., Model "Dilatronic 9" dilatometer. This is a two-pushrod apparatus in which parallel horizontal rods of fused silica, 1 cm apart, are used. One rod contacts a fused silica standard; the other contacts the sample being analyzed. The pushrods, which extend out of the clamshell furnace used for heating the sample and standard, are connected to two linear displacement transducers. The sample is ground equal in length to the silica standard  $\pm 0.18$  mm. Nominal sample length is 2.54 cm; shorter samples can be analyzed since available standards range from 1.27 to 2.54 cm. The heating rate of the furnace is programmable to rates of between  $0.5^\circ$  and  $10^\circ\text{C}/\text{min}$ . Because the system is not actively cooled, cooling rates are limited (especially at lower temperature) by the rate of heat loss from the furnace and sample/standard/pushrod assembly. Sample temperature is measured by a Chromel-Alumel thermocouple placed at the lengthwise midpoint of the sample and halfway between the sample and silica standard. Estimated maximum error of the sample temperature measurement is  $\pm 5^\circ\text{C}$ ; errors at slow heating rates are probably much smaller.

Output during measurement consists of a digital display of measured sample temperature and a continuous graph of the change in sample length as a function of temperature ( $^\circ\text{C}$ ) relative to the net change in length of the fused silica standard to the same temperature. Plotted and digital readout temperatures are cross-checked periodically during runs and agree to within  $5^\circ\text{C}$ . It is the chart record that is preserved and from which expansion coefficients are calculated.

Samples used in these measurements are, when possible, taken from core material that was protected by wax and wrapped as soon as possible after removal from the ground. Blanks are rough-cut to 5 mm x 5 mm x 3 cm on a water-cooled saw and, if necessary, stored in tap water before analysis. Just before measurement, samples are ground to the desired initial length and squared on a water-cooled lapidary wheel, using a machinist block for alignment. This process usually requires only 1 to 2 min per sample. Sample length before analysis is measured with a mechanical caliper (measurements reproducible to  $\pm 0.05$  mm) and recorded on the record chart; the ends of the sample are wiped dry and the sample is placed in the dilatometer for expansion measurement.

For this report, average linear expansion coefficients are calculated as follows:

1. Total changes of sample length relative to standard length ( $\Delta L$  graph) are recorded over a given temperature interval.
2. The relative expansion coefficient of the sample between  $T_1$  and  $T_2$  ( $\alpha_{T_1 - T_2}^{rel}$ ) is calculated from

$$\alpha_{T_1 - T_2}^{rel} = \frac{\Delta L_{\text{graph}}}{(T_2 - T_1)L_0},$$

where  $L_0$  is the initial sample length.

3. The final coefficient of the sample ( $\alpha_{T_1 - T_2}^{fin}$ ), corrected for expansion of the fused silica standard, is calculated from

$$\alpha_{T_1 - T_2}^{fin} = \alpha_{T_1 - T_2}^{rel} + \alpha_{T_1 - T_2}^{sil},$$

where  $\alpha_{T_1 - T_2}^{sil}$  is the average linear thermal expansion of fused silica over the range  $T_1 - T_2$ .<sup>5</sup> Table I shows representative values and also

temperature intervals over which expansion is generally averaged.

TABLE 1

Ambient-Pressure Linear Thermal-Expansion Coefficients  
of Fused Silica as a Function of Temperature<sup>3</sup>

$\alpha(10^{-6}\text{ }^{\circ}\text{C}^{-1})$	T ( $^{\circ}\text{C}$ )
0.50	20-100
0.60	100-200
0.55	20-200
0.62	200-300
0.60	20-300
0.57	300-400
0.51	400-500
0.57	20-500

#### Precision and Accuracy of Measurements

Four obvious factors may affect the precision of the measurements reported here:

1. Recorded sample temperatures may be affected by thermal gradients within the dilatometer apparatus and by uncertainties in reading the chart record. Although reported temperatures are generally felt to be good to  $+5^{\circ}\text{C}$ , this may not be true at high heating rates ( $5^{\circ}$  to  $10^{\circ}\text{C}/\text{min}$ ) because of the presence of thermal gradients within the sample.
2. The recorded initial sample length is accompanied by a small uncertainty, as discussed above.
3. Initial heating rates (i.e., at temperatures below  $35^{\circ}\text{C}$ ) are somewhat uncertain because the sample temperature and initial furnace ramp temperature for heating are matched mechanically by adjusting the ramping temperature upwards until a minimal furnace output is required. This may result in over- or underheating for a short time, depending on the heating rate. Effects of this uncertainty are not evident unless the length of the test sample changes because of dehydration near room temperature.

4. Sample inhomogeneities may play a major role in limiting the precision of measurements on fairly small samples, especially in rocks that contain xenoliths or pumice fragments of the same size scale as the samples being measured. In order to make a limited test of sample inhomogeneity effects and general precision, triplicate measurements were made at a constant heating rate of 1°C/min on two samples containing abundant xenoliths and inhomogeneities, GTEv6#3-115 (welded) and GTEv3#11-35 (nonwelded). These measurements indicate that measured expansion coefficients are precise to about  $\pm 1 \times 10^{-6} \text{ } ^\circ\text{C}^{-1}$ , but do not include effects of inhomogeneities larger than the samples analyzed.

Two main factors may affect the accuracy and applicability of these data--accuracy of instrumental calibration and inherent limitations in the interpretation and use of ambient-pressure data collected on materials that were under in-situ stress before removal to the surface. Calibration of the dilatometer used in making these measurements is checked by weekly measurement of the linear expansion of 99.99%-pure Pt metal to 500°C. Analysis of 18 such runs yields an average net linear strain and expansion coefficient to 500°C of  $0.4580 \pm 0.0001$  and  $9.543 \pm 0.003 \times 10^{-6} \text{ } ^\circ\text{C}^{-1}$ , compared with National Bureau of Standards (NBS) reference values of 0.4592 and  $9.57 \times 10^{-6} \text{ } ^\circ\text{C}^{-1}$ , respectively.<sup>6</sup> These results indicate accuracy of machine calibration to within ~0.3%.

Thermal expansion coefficients reported here are based on measurements of total changes in sample length and therefore include effects of reversible and irreversible mineralogic transformations, in addition to changes in rock fabric (i.e., the opening or closing of microcracks and/or pores). The mineralogic transformations of greatest interest involve dehydration of clays, hydrated silicic glass and/or zeolites, all of which are distinctly pressure-dependent, and changes in silica polymorph crystallography.

In general, two types of pressure must be considered in extrapolating a mineral reaction to depth--the pressure upon the solid phases in a system ( $P_s$ ) and that effective in confining the fluid within a system ( $P_f$ ).

This is especially true with dehydration reactions. Data reported here are collected under conditions of  $P_s = 0.1$  MPa and  $P_f = 0$  MPa. At depth, a variety of conditions are possible at a general total stress level ( $S$ ) from  $P_s = P_f = S$  to  $P_s = S$ ,  $P_f = 0$ . Relative fluid and solid pressures anywhere near a repository at depth would depend upon the relationship between local fluid permeabilities, heating rates, and fluid-release path lengths. Therefore, based on measurements made here, extrapolation of dehydration reactions to repository depth will rely upon assumption or calculation of relative fluid and solid pressures at the depths of interest. This approach is being actively pursued, but is beyond the scope of this report.

Cooper and Simmons<sup>7</sup> have shown that ambient-pressure thermal expansion coefficients may be affected considerably by the presence of both pre-existing microcracks and cracks generated by expansion mismatches of constituent grains during heating. Microcracks may be present at ambient temperature because of several factors. If the rock is quartz- or cristobalite-bearing and has cooled through the  $\beta \rightarrow \alpha$  transition temperatures for either of these phases, significant microcracking is almost certain to be present at ambient temperature unless cooling was slow enough to allow annealing. Microcracking may also result from removal of samples from in-situ to surface environments because of mismatched compressibilities of constituent grains.

Preexisting microcracks should lead to initial ambient-pressure expansion coefficients that are lower than at high pressure, since part of the expansion of constituent grains can be taken up by expansion into existing microcracks. Generation of microcracks because of mismatched thermal expansion of constituent grains should lead to apparent expansion values that increase with temperature more rapidly than do the coefficients of the constituent grains. Wang and Brace<sup>8</sup> have recently shown that effects caused by the presence of microcracks can persist to confining pressures of up to 200 MPa, depending upon rock type and sample thermal history.

While the extrapolation of dehydration reactions to depths is feasible and relatively straightforward (given knowledge of in-situ fluid pressures), the effects of microcracks are not. Thus, the expansion

measurements reported here must be considered only as qualitative and should not be applied quantitatively to repository depths. Quantitative laboratory evaluation of the thermal expansion of tuffs at depth will require the development of techniques to make measurements at known fluid pressures and effective confining pressures. Full evaluation of the behavior of tuff masses upon heating can only be made by in-situ testing.

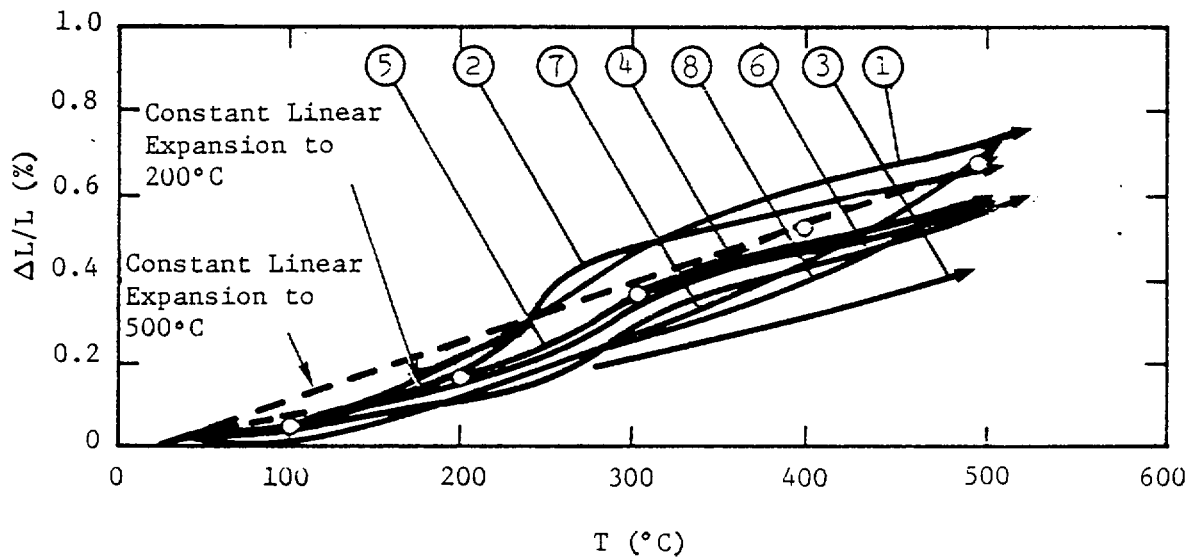
## Results

### Expansion Behavior of Devitrified Welded Tuffs

As mentioned above, a major inherent variable of silicic tuffs is porosity. Within ash-flow sheets, variable porosity results from differing degrees of compaction of the initial fragmental debris cloud and from secondary processes such as devitrification and alteration. In this report, it is assumed that the final sample porosity rather than the initial degree of welding controls sample behavior. Rocks are therefore grouped according to their final porosity (which is measurable) rather than by their initial degree of welding (which can only be estimated qualitatively). However, there is a general correlation between final porosity and degree of welding. Tuffs with a final porosity of 25% or less are considered welded; those with a porosity of greater than 25% are considered nonwelded. All porosities in this report were measured or calculated after heating the sample to between 105° and 110°C.

From an engineering point of view, the most striking feature of the ambient-pressure thermal expansion of devitrified welded tuffs is the degree of uniformity of the results, regardless of sample source, porosity, and mineralogy. Figure 2 shows changes in length of eight samples of welded tuff relative to fused silica as a function of temperature to 500°C. Table 2 summarizes numerical data for these same samples, and Table 3 summarizes available material properties data for all samples.

As Figure 2 and Table 2 indicate, an "average" devitrified welded tuff displays a gradually increasing expansion coefficient to at least 300°C. Care must be taken to consider this variability when using a constant  $\alpha$  for mechanical modeling. Use of a constant  $\alpha$  based on measurements to 500°C (or even 200°C) tends to overestimate expansion and, hence, stresses and displacements at lower temperatures. The significance of non-linearity in the behavior of an "average" welded tuff in thermomechanical modeling depends upon the degree of accuracy required.



	<u>Porosity (%)</u>
1 Ue25A#1-166	7.5
2 Ue25A#1-186	24.5
3 JA-13	----
4 GTEv6 #3-68	----
5 GTEv6 #3-80	----
6 GTEv6 #3-115	14.6
7 Ue25A#1-2494	18.2
8 JA-29	----
o Average expansion of eight samples to indicated temperature	

Figure 2. Relative Linear Thermal Expansion of Eight Devitrified Welded Tuffs to 500°C (Heating Rate = 1°C/min)

TABLE 2

Linear Thermal Expansion Coefficients of Devitrified Welded Tuffs ( $\alpha = 10^{-6} \text{ } ^\circ\text{C}^{-1}$ )  
(Heating Rate =  $1 \text{ } ^\circ\text{C}/\text{min}$ )

Sample	Number of Measurements	Temperature Interval ( $^\circ\text{C}$ )							
		amb-100	100-200	amb-200	200-300	amb-300	300-400	400-500	amb-500
Ue25A#1-166	2	9.0	15.9	12.5	24.4	17.2	18.6	11.5	16.0
Ue25A#1-186	2	6.8	13.6	10.6	29.9	17.5	9.4	9.8	14.2
JA-13	2	5.8	8.8	7.5	8.9	7.9	10.6	13.5	9.7
GTEv6#3-68	2	8.0	12.6	10.6	19.1	13.8	16.1	13.0	13.9
GTEv6#3-80	2	7.8	10.1	9.1	16.9	11.9	14.9	13.2	12.8
GTEv6#3-115	6	6.7	8.4	7.8	15.7	10.6	16.6	15.4	12.9
Ue25A#1-2494	3	4.0	10.3	7.5	14.0	9.9	18.5	25.8	15.1
JA-29	2	6.8	10.6	8.9	11.6	9.9	15.6	20.5	13.3
$\bar{X}$ all	21	6.9	11.3	9.3	17.6	12.3	15.0	15.3	13.5
$1 \sigma$ all		1.5	2.6	1.8	6.9	3.5	3.4	5.3	1.9

TABLE 3

## Available Bulk Properties Data\*

Sample Location Depth (ft)	Bulk Density (g/cm <sup>3</sup> )	Grain Density ( $\rho_g$ g/cm <sup>3</sup> )	Porosity		Weight (% H <sub>2</sub> O)	Saturation
			Calculated	Measured		
<u>Ue25A#1</u>						
166	2.40	2.52	7.5	--	3.1	--
186	2.12	2.48	24.5	--	11.6	--
212	1.66	2.30	49.3	--	29.8	--
723**	2.33	2.56	12.9	12.8	4.0	0.80
1290	2.33	2.40	3.7	--	--	--
1490	1.99	2.42	28.1	29.1	12.2	0.86
1544	1.95	2.43	34.0	--	17.0	--
1555	1.94	2.46	32.6	28.0	14.9	0.89
1561	1.95	2.48	33.5	30.3	15.6	0.91
1605	1.93	2.37	20.5	28.9	13.8	0.90
1662	1.87	2.38	34.9	34.1	17.1	0.91
1861						
1949	2.32	2.63	18.4	18.6	7.5	0.95
1968	2.28	2.61	18.0	20.9	6.0	0.76
1978	2.34	2.62	16.9	17.0	6.9	0.95
1981	2.36	2.63	16.0	--	7.0	--
1985	2.36	2.62	14.5	15.8	5.1	0.83
2402	2.28	2.61	19.2	20.7	7.5	0.89
2423	2.23	2.62	23.6	23.7	10.3	0.98
2432	2.33	2.64	18.2	18.1	7.5	0.96
2453	2.23	2.61	20.3	24.2	7.1	0.78
2492	2.30	2.60	17.7	20.8	6.9	0.90
2494	2.34	2.64	18.2	--	7.8	--
<u>G-Tunnel</u>						
Ev6#3-115	2.36	2.58	14.6	--	6.4	--
Ev6#1-181	1.69	2.20	42.8	--	25.2	--
Ev6#11-35	1.96	2.50	35.6	--	18.1	--
<u>Well J-13</u>						
JA-6	2.37	2.52	8.1	--	--	--
JA-13	2.41	2.64	12.3	--	--	--
JA-22	2.00	2.45	29.9	--	--	--
JA-29	2.23	2.62	20.3	--	--	--

\*In some cases, data are for sample near one on which expansion was measured.

\*\*Entries including sample saturation are from References 9 and 10; all other are from unpublished data.

In addition to the general nonlinearity in thermal expansion of devitrified welded tuffs, two distinctive mineralogic effects are shown by some samples (Figure 3). Sample Ue25A#1-186 from the Tiva Canyon Member of the Paintbrush Tuff displays a marked nonlinearity between 220° and 270°C on heating, and 230° to 180°C on cooling because of the presence of cristobalite. Cristobalite is the major silica polymorph that results (along with alkali feldspars) from simple devitrification of vitrified tuffs.<sup>11</sup> It occurs mostly in shallower, younger units, such as the Tiva Canyon tuff, and is replaced by quartz in deeper, older tuffs such as the Bullfrog Member of the Crater Flat Tuff from which sample Ue25A#1-2494 was taken. Since the phase relations of cristobalite are quite complex and could be of concern if any cristobalite-bearing tuff were heated above ~200°C as a result of emplacement of nuclear waste, they are briefly discussed here.

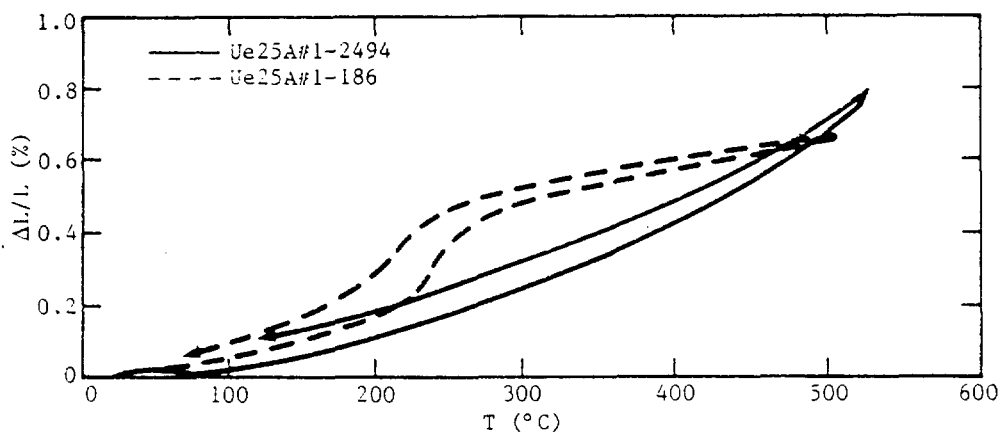


Figure 3. Relative Linear Thermal Expansion of Samples Ue25A#1-186 and Ue25A#1-2494, Both Devitrified Welded Tuffs (Heating Rate = 1°C/min)

Upon heating, cristobalite inverts over some temperature range from a low-temperature tetragonal form ( $\alpha$  cristobalite) to a cubic form ( $\beta$  cristobalite) stable at high temperatures. The most recent compilation of thermodynamic data for geologic materials<sup>12</sup> assigns a temperature of 250°C to the  $\alpha$ - $\beta$  transformation of cristobalite. However, as Sosman discusses,<sup>13</sup> the temperature of the transformation and the volumetric increase accompanying it depend upon either the last (lowest) temperature at which the

cristobalite was annealed or the temperature of formation in unannealed samples. For example, cristobalites formed at temperatures of 850° and 1600°C complete inversion on heating at temperatures of 200° and 275°C, respectively. Inversion is defined as that point where the X-ray morphology changes from tetragonal to cubic symmetry, and occurs at the high-temperature side of the volumetric changes. Volumetric change during the  $\alpha$ - $\beta$  cristobalite transformation ranges from 2.1% to 3.3%, with samples formed at higher temperatures displaying the larger volume changes. A final point of interest regarding the transformation is that it shows a heating rate-independent hysteresis, with transformation temperatures during cooling 16° to 40°C lower than on heating.<sup>13</sup> Samples equilibrated at higher temperatures display a more marked hysteresis of inversion temperature. The cristobalite in Sample 186 completes inversion at about 260°C on heating, with an inversion hysteresis of 25°C. Because of the presence of cristobalite, Sample 186 has a measured  $\alpha_L$  between 230° and 260°C of  $57 \times 10^{-6} \text{ } ^\circ\text{C}^{-1}$ , compared with  $13 \times 10^{-6} \text{ } ^\circ\text{C}^{-1}$  for Sample 2494, which lacks this phase.

Note that the presence or absence of cristobalite in a welded tuff appears to have a major effect on thermal expansion only at temperatures greater than 200°C. Because of this temperature limitation, the presence or absence of cristobalite would be expected to have only a very limited effect upon waste disposal except at higher power densities and temperatures.

Sample Ue25A#1-2494, though it contains no detectable cristobalite, contains small amounts of biotite, which characteristically makes up as much as 2% of the Crater Flat Tuff.<sup>4</sup> Mafic silicate phenocrysts in ash-flow tuffs, especially hornblende and biotite, are frequently altered as a result of deuteritic or vapor-phase alteration, much of which is inherent to processes of degassing soon after emplacement.<sup>14</sup>

Figure 3 shows that Sample Ue25A#1-2494 contracts a very slight amount ( $\approx 0.03\%$  by volume) between 50° and 75°C, after expansion by approximately the same amount between ambient temperature and 50°C. This contraction, which has been noted in all blanks of this sample that have been

analyzed, is probably because of dehydration of small amounts of expandable clay present as a result of alteration of the biotite. Preliminary thin-section examination of this sample indicates a content of 1% to 2% by volume biotite with minimal alteration. If it is assumed that the observed contraction in this sample stems from the collapse of the basal spacing of vermiculite and/or montmorillonite interlayers in the biotite from 15 Å to 10 Å upon dehydration, and that the biotite content of this rock is 1% by volume, then only 10% of the biotite need be altered to one of these expandable phases to account for the observed behavior.

This result suggests that small degrees of alteration of the biotite in biotite-bearing welded tuffs can greatly affect the expansion of such tuffs near the boiling point of water, and could lead to smaller expansions and displacements than those expected in a similar tuff free of biotite. As an example, for a tuff with 2% biotite and a subboiling  $\alpha_L$  of  $10 \times 10^{-6} \text{ } ^\circ\text{C}^{-1}$  to return to its initial volume after dehydration near 100°C, the biotite needs to be altered 35% to 40% to an expanding phase, the basal spacing of which collapsed from 15 Å to 10 Å upon dehydration. Thus 0.8% by volume of expandable phase would completely dominate the total expansion of this material to just above 100°C. Increased in-situ fluid pressures would raise the boiling points of water, and hence the temperature at which clay contents became critical. Very small variations in biotite content, or in degree of alteration, could thus significantly affect predictions of near-field stresses and displacements resulting from waste emplacement in biotite-bearing tuffs. Thus, for applications at temperatures below about 200°C, the single most critical mineralogic factor in predicting the matrix expansion of devitrified welded tuffs is a careful analysis and measurement of the degree and type of alteration of mafic silicates (and especially biotites) that those tuffs might contain. In addition, such predictions will require a good estimate of the fluid pressure actually present in any waste management application, since this controls the temperature at which the expandable phases dehydrate.

The possibility of anisotropic thermal expansion of welded tuffs has been examined by multiple measurements on mutually perpendicular blanks; the results are summarized in Table 4. Based on these results, there

appears to be no significant directional dependence of the ambient-pressure linear expansion of devitrified welded tuffs.

TABLE 4

Linear Thermal Expansion of Devitrified Welded Tuff GTEv6#3-115  
 $(\alpha_L \text{ in } 10^{-6} \text{ } ^\circ\text{C}^{-1})$  (Heating Rate =  $1^\circ\text{C}/\text{min}$ )

	Temperature Range ( $^\circ\text{C}$ )						
	amb-100	100-200	200-300	amb-300	300-400	400-500	amb-500
<b>Perpendicular to Bedding</b>							
<u>Run</u>							
1	6.9	8.6	17.6	11.4	17.6	15.5	13.6
2	6.3	8.6	16.6	10.4	16.6	15.5	12.6
3	5.6	8.1	15.1	9.9	17.1	14.0	12.3
X	6.3	8.4	16.1	10.6	17.1	15.0	12.8
1	0.7	0.3	1.3	0.8	0.5	0.9	0.7
<b>Parallel to Bedding</b>							
<u>Run</u>							
1	7.0	8.6	15.6	10.6	16.5	15.5	13.0
2	7.8	8.6	15.6	10.9	15.5	17.5	13.7
3	6.8	8.1	14.6	10.1	16.1	14.5	12.3
X	7.2	8.4	15.3	10.5	16.1	15.8	13.0
1	0.5	0.3	0.6	0.4	0.5	1.5	0.7

#### Expansion Behavior of Vitric Welded Tuffs and Obsidians

Measurements indicate that expansion of devitrified welded tuffs is fairly predictable and uniform, though greatly affected by the presence or absence of expandable clays and cristobalite. Limited results on vitric welded tuffs and obsidians indicate a more complex, less uniform behavior and suggest that the presence or absence of hydrated silicic glasses may be a major parameter to be considered in tuffs heated above the boiling point of water, just as is the presence or absence of expandable clays. Although many nonwelded tuffs examined as part of this study contain silicic glass, only the vitric welded tuffs and obsidians are considered in this section. A few of these are almost entirely glassy and offer some understanding of the behavior of natural silicic glass itself.

The silicic glass in fresh, unaltered tuffs usually contains only a few tenths of a percent water, which is entrapped in the melt at high temperature and actually forms part of the silicate network within the glass.<sup>15</sup> Driving off such water at relatively high temperatures should cause the glass to contract, since water is an integral part of the melt structure and has a positive partial molar volume.<sup>16</sup> Silicic glasses, especially those in older tuffs, are often additionally hydrated by interaction with groundwater at deuteric or ambient temperatures. Total water contents of up to 7% by weight are not uncommon.<sup>3 17</sup>

The volumetric effects of the addition of this water at low temperature are not well understood. For example, Hoover<sup>3</sup> argues that hydration occurs at constant glass volume, with the addition of water compensated for by leaching of cations, especially Na. However, there is considerable scatter in the data he uses to support this argument. Ross and Smith<sup>15</sup> also state that the volumetric changes upon hydration are small. The fact that cores of nonhydrated obsidian in perlite are separated from rims of hydrated obsidian by concentric cracks<sup>15</sup> suggests, however, that some increase in glass volume during hydration is likely at lower temperatures and, hence, this glass will contract if dehydrated.

Three samples have been examined as part of this study in an attempt to unravel this uncertainty. Sample Ue25A#1-1290 from the basal vitrophyre of the Topopah Springs Member of the Paintbrush Tuff contains abundant black glass but is partially and irregularly altered to a very fine-grained, orange alteration product. The detailed nature of this product is still unclear, but it contains both glass and a zeolite (heulandite). The character of this unit in Hole Ue25A#1 is very similar to its appearance in Well J-13, some 6 mi distant.<sup>18</sup> Two samples of obsidian were also studied as examples of less-altered material.

Thermogravimetric analyses of the two obsidians and of both the most- and least-altered parts of Ue25A#1-1290 were run on a standard apparatus (DuPont Model 990) to examine volatile evolution behavior. The two obsidians either contain no water or water below detectable levels. Both

portions of Sample Ue25A#1-1290, however, contain abundant water. The relatively unaltered portion of this sample retains about 4% by weight of water after powdering for analysis. This is evolved discontinuously, since most water (3% by weight) is released above 200°C (Figure 4). This sample thus appears to have been hydrated predominately at relatively high temperatures, probably by deuteric action. The more altered portion of Sample 1290 contains 10% by weight of water, which is evolved continuously to 400°C; almost half of it is driven off by 100°C. This type of water evolution is consistent with the presence of heulandite or clinoptilolite in this sample. Figure 4 also shows thermal expansion results for the same samples.

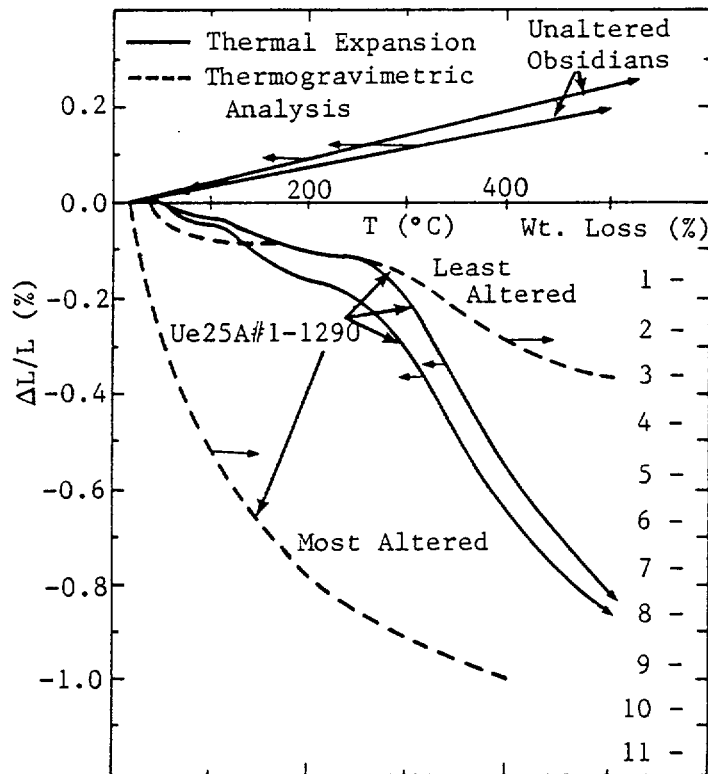


Figure 4. Relative Linear Thermal Expansion of Two Obsidians and Sample Ue25A#1-1290. (Also shown are thermogravimetric results for Sample 1290; heating rate for expansion = 1°C/min, for TGA = 2°C/min)

Thermal expansion of the unaltered obsidians, assumed here to be equivalent to the behavior of nonhydrated or slightly hydrated silicic glass,

is markedly different from the behavior of crystalline tuffs. Both obsidians show strictly linear behavior with temperature as opposed to the general increase in  $\alpha_L$  with T shown by the crystalline tuffs. The obsidians display no hysteresis upon cooling, again in contrast with the devitrified tuffs (Figure 3). The distinction between the behavior of obsidian and of devitrified tuff is consistent with the interpretation that at least part of the increase in  $\alpha_L$  with T in crystalline rock results from microcracking caused by the mismatch of individual grains.<sup>7</sup> The average  $\alpha_L$  to 500°C for the two obsidians analyzed is  $5.0 \times 10^{-6} \text{ } ^\circ\text{C}^{-1}$ , as opposed to  $13.5 \times 10^{-6} \text{ } ^\circ\text{C}^{-1}$  for analyzed devitrified welded tuffs.

Correlation of thermogravimetric and expansion results for Sample 1290 suggests that dehydration of natural glasses, especially at temperature above 300°C, measurably decreases glass volume. Figure 4 shows only minor contraction of Sample 1290 below 150°C, by which time the altered portion of this sample (which makes up some 10% by volume of the rock) has evolved 2/3 of its water. The major increase in contraction rate of Sample 1290 correlates well with increased water evolution from the least-altered part of this sample. This is indicated by the fact that the major inflection in the thermogravimetric data for this portion and the major increase in contraction rate for the sample as a whole both occur near 300°C. The sample still needs to be studied in detail to determine the dehydration/expansion response of the separate phases within the most altered portion.

From these data, it is tentatively concluded that almost all hydration of natural silicic glasses results in at least some increase in glass volume; dehydration of such glasses should lead to contraction with hysteresis on cooling, as seen in Sample 1290. Water evolution from such glasses is highly variable, but becomes increasingly continuous and shifts to lower temperatures as the total water content increases. Thus the evolution of water at temperatures near 300°C appears to be associated with major contraction. It has not yet been possible to measure the effects of water evolution near 100°C, although results suggest that removal of this more poorly retained water also leads to limited contraction. Certainly, disposal of nuclear wastes in a situation in which glass-bearing tuffs

reach temperatures above the boiling point would be advised only if the time-temperature-fluid pressure-volume relations of hydrated silicic glasses were much better understood than at present.

#### Expansion Behavior of Nonwelded Tuffs

As emphasized by the results shown in Figure 2, expansion of welded tuffs appears to be independent of porosity. The extreme variability of expansion results for nonwelded tuffs, discussed below, requires consideration of possible porosity effects. If it is assumed that no cracks develop during expansion of an aggregate (i.e., that the individual grains are tightly bound to each other and that there are no shear stresses), the linear expansion of the aggregate can be approximated by<sup>19</sup>

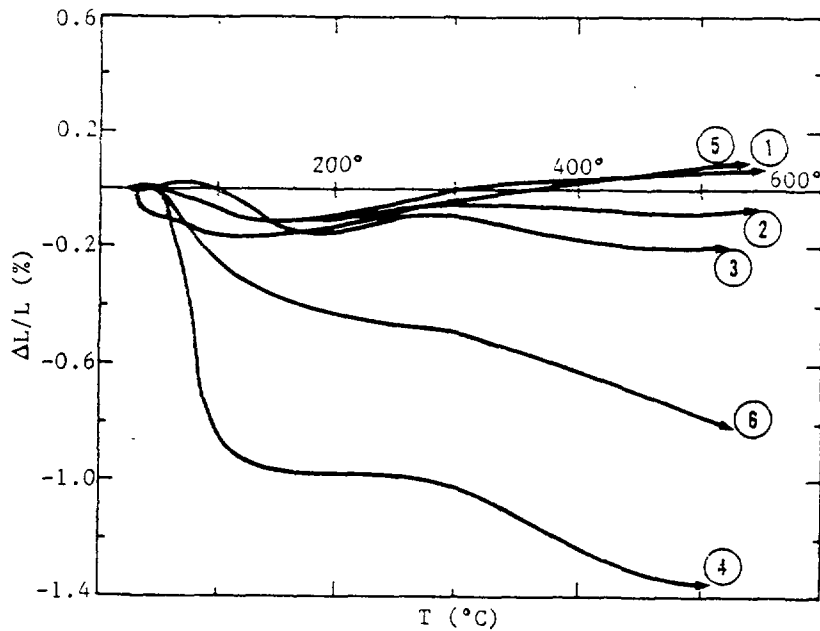
$$\alpha_r = \frac{\alpha_1 K_1 F_1 / \rho_1 + \alpha_2 K_2 F_2 / \rho_2 \dots}{K_1 F_1 / \rho_1 + K_2 F_2 / \rho_2 \dots}$$

where

- $\alpha_r$  = expansion coefficient of the aggregate
- $\alpha_i$  = expansion coefficients of the  $i^{\text{th}}$  phase
- $K_i$  = bulk modulus of the  $i^{\text{th}}$  phase
- $F_i$  = weight fraction of the  $i^{\text{th}}$  phase
- $\rho_i$  = density of the  $i^{\text{th}}$  phase

Air-filled or unsaturated porosity can be simply treated as another phase in this formalism, a phase with a negligibly low-bulk modulus. Therefore, in theory, the presence of porosity should have no effect upon thermal expansion so long as the assumptions given above are valid.

Results of measurements on nonwelded tuffs, shown graphically in Figure 5 and summarized numerically in Table 5, indicate general contraction between 100° and 300°C for tuffs with greater than 25% porosity. All the nonwelded tuffs studied to date contain some clay mineral, apparently montmorillonite; many contain clay minerals, silicic glass, and zeolite (clinoptilolite or heulandite). In general, highest-porosity samples contract most. Although this is inconsistent with intuition based on the above arguments, it is consistent with the generally observed increase in mineralogic complexity in the more porous samples.



	<u>Porosity (%)</u>
1 Ue25A#1-1561	30
2 Ue25A#1-1544	34
3 JA-22	30
4 Ue25A#1-212	49
5 GTEv3#11-35	36
6 GTEv#3-181	43

Figure 5. Relative Linear Thermal Expansion of Six Nonwelded Tuffs to 500°C (Heating Rate = 1°C/min)

TABLE 5

Linear Thermal Expansion Coefficients of Nonwelded Tuffs ( $\alpha = 10^{-6} \text{ } ^\circ\text{C}^{-1}$ )

Sample	Heating Rate (°C/min)	Temperature Interval (°C)						
		amb-100	100-200	200-300	amb-300	300-400	400-500	amb-500
Ue25A#1-212	1	-69.9	-11.5	-5.6	-25.2	-20.7	-11.1	-21.2
GTEv6#1-181	1	-24.0	-20.7	-5.5	-16.2	-10.3	-14.0	-14.5
(1 $\sigma$ of 4 measurements, Sample 181)		1.5	1.2	0.6	0.8	0.3	0.7	0.6
GTEv3#11-35	1	-20.5	+3.8	+10.1	-0.7	+5.6	+4.5	+1.7
(1 $\sigma$ of 3 measurements, Sample 35)		1.1	1.0	0.5	0.1	0.5	0.5	0.3
JA-22	5	0.7	-12.6	+4.6	-2.7	-4.7	-4.3	-3.4
Ue25A#1-1544	1	-9.4	-2.2	+6.3	-1.1	+0.8	-0.7	-0.6
Ue25A#1-1561	1	-9.1	-0.7	+9.9	+1.0	+4.4	+3.2	+2.3

The rough correlation of high porosity and mineralogic complexity evident from studies to date appears to be related to tuff genesis. The predominance of silicic glass in both the highly porous nonwelded tuffs and in the low-porosity basal vitrophyre of the Topopah Springs appears to be a result of the facts that (1) glass in the nonwelded tuffs was originally emplaced at relatively low temperatures, either as ash-fall debris, or as cool (and hence nonwelded) margins on an ash-flow sheet; and (2) the basal vitrophyre portion of an ash-flow sheet, though quite hot at the time of emplacement and hence very densely welded, is cooled quite rapidly, often before devitrification can occur.<sup>11 14</sup> In addition, the very low porosity of the vitrophyre itself should limit the deuteric action that might enhance devitrification. The apparent predominance of clay materials in the nonwelded tuffs also appears to be related to their original high porosity and glass content. In general, the normal alteration sequence of natural silicic glasses is hydration and leaching by interaction with groundwater or pore fluids,<sup>3 20</sup> followed by alteration of their rims to either zeolites or, more commonly, montmorillonite.<sup>3 21</sup> Thus, the widespread occurrence of clays and zeolites in the nonwelded rocks studied here appears to be directly related to their original glass contents and is not an isolated phenomenon.<sup>14</sup>

Two series of tests were run to make a preliminary evaluation of the effects of differing heating rates on the thermal expansion behavior of tuffs. Cyclic measurements of expansion of one welded tuff (GTEv6#3-115) at heating rates of from 0.5° to 10°C/min indicated no statistically significant variations in expansion rate, either as a function of initial heating rate or as a function of previous sample history. Measurements on a high-porosity nonwelded sample (GTEv6#1-181) support the interpretation that expansion/contraction of nonwelded samples is a strong function of dehydration reactions and, hence, of fluid pressure (Figure 6). The temperature at which the first major contraction begins on initial heating is consistently proportional to the heating rate, as is the total sample contraction. After reheating, sample contraction is greater in more rapidly

heated samples. These results are further evidence of the potential complexities in waste-management activities resulting in significant heating of nonwelded tuffs.

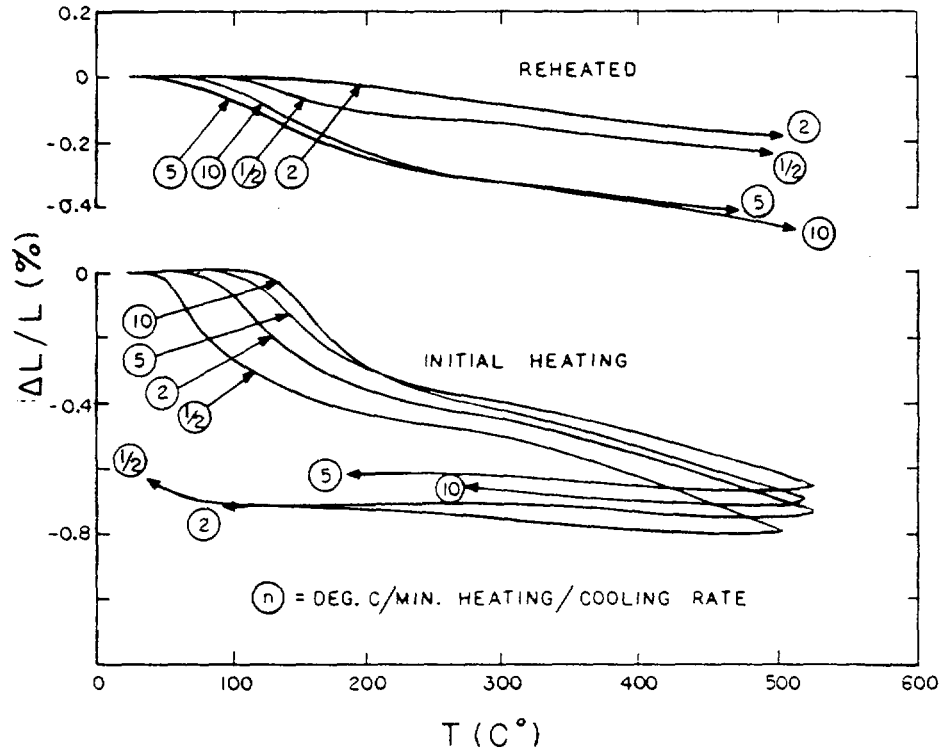


Figure 6. Heating Rate Dependence of Relative Linear Thermal Expansion, Sample GTEv6#1-181

Measurements to date on nonwelded tuffs indicate that at least three major factors need to be much better defined before their behavior at depth can be understood. Porosity collapse, which appears not to be a factor in expansion of welded tuffs, may play a major role in in-situ reponse of nonwelded tuffs. Determination of this effect is likely to be complicated by an additional correlation of increased mineralogical complexity with increasing porosity. This correlation appears at present to be related directly to the genesis of high-porosity tuffs. As shown by preliminary heating-rate experiments, the high-water content and mineralogical complexity of nonwelded tuffs result in their expansion behavior being dependent on fluid pressure.

One entire class of minerals (zeolites) that is quite widespread in silicic tuffs and related sediments<sup>3 22</sup> has not been considered here. Some of the nonwelded samples studied contain appreciable zeolite, especially Ev6#1-181, Ev3#11-35, JA-22, and samples from near the 1500-ft level of Ue25A#1. The predominant zeolite in these samples is clinoptilolite. Other zeolites reported at NTS<sup>3</sup> or in the J-13 well<sup>18</sup> include chabazite, analcime, mordenite, erionite, phillipsite, and heulandite. The extent of the distribution of zeolites other than clinoptilolite and analcime is minor. Table 6, modified from Reference 23, summarizes the available differential thermal analysis, thermogravimetric analysis, and structural stability data for these minerals.

As shown, the evolution of water from these zeolites, except for phillipsite and heulandite, is continuous and results in no structural changes, shrinkage, or instability to temperatures as high as 750°C, at least on a short-term basis. It is therefore concluded that the major effect of variable zeolite contents in tuffs (except for phillipsite and heulandite) is to vary the water-evolution history and hence fluid-pressure history in the heated area rather than to vary the expansion response directly. As shown by Sample Ue25A#1-1290, however, the presence of heulandite directly affects expansion. Note that the above conclusion also assumes that the zeolites have no significant effect on the elastic and mechanical properties of a given tuff.

#### Conclusions and Discussion

The primary goal of this report is to present preliminary data on the ambient-pressure thermal-expansion behavior of a broad range of tuffs. Figure 7 shows the general range of tuffs examined to date and indicates the average linear expansion coefficient to 200°C of all samples analyzed, as a function of final sample porosity.

TABLE 6

Thermal, Thermogravimetric, and Structural Data for the Most Common Zeolites in Silicic Tuffs\*

<u>Type of Zeolite and Comments</u>	<u>DTA</u>	<u>TGA</u>	<u>Structural Stability</u>
Clinoptilolite	Endotherm, 125° to 300°C	Continuous; $\Sigma$ 14%	Stable to at least 750°C
Analcime (major, especially at depth)	Endotherm, 200° to 400°C	Continuous weight loss to 400°C; $\Sigma$ 8.7%; dehydration reversible	Stable to 700°C
Mordenite, not uncommon	Endotherm, 25° to 300°C	Continuous; $\Sigma$ 16%	Stable to at least 800°C
Erionite, minor	Endotherm, 50° to 400°C	Continuous; $\Sigma$ 15%	Stable to at least 750°C
Heulandite traces; some old literature reports clinoptilolite as heulandite	Endotherm, 25° to 300°C; discrete at 350°C	Stepwise weight loss, near 100° and 250°C; $\Sigma$ 17%	Transforms to heulandite "B" near 250°C; structure collapses above 360°C; some lattice contraction to 180°C the start of transformation
Phillipsite, traces	Endotherms at 100°, 200°, 300°C	Stepwise weight loss, starting near 130°C; $\Sigma$ 18% @ 300°C	New structure forms at 160° to 200°C; small change, "metaphillipsite"
Chabazite, minor	Endotherm, 25° to 300°C	Continuous; $\Sigma$ 23%	Stable to at least 700°C

\*Modified from Reference 23

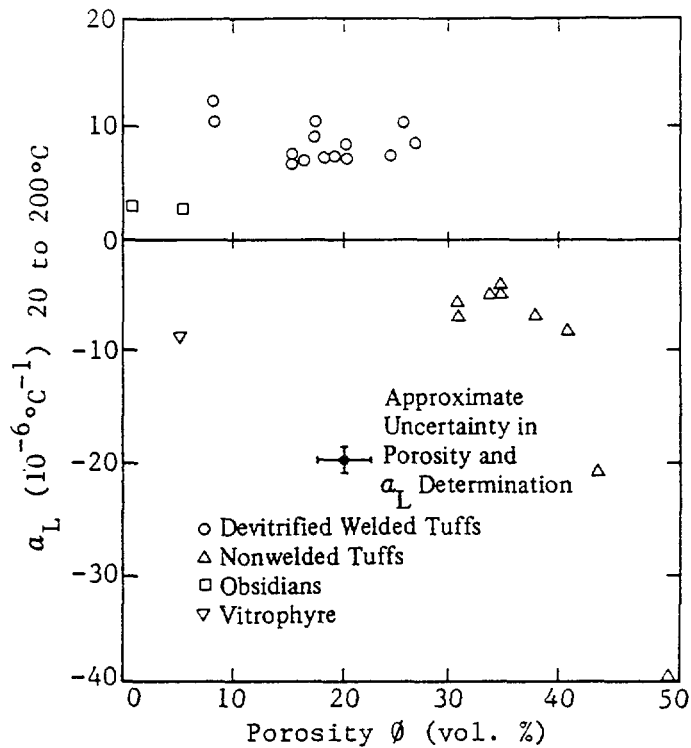


Figure 7. Linear Expansion Coefficient to 200°C vs Final Porosity of Analyzed Tuffs and Obsidians

Devitrified welded tuffs, analyzed samples of which have final porosities of between 8% and 26%, are fairly uniform in behavior to 200°C; the  $\alpha_L$  for all 14 such samples analyzed is  $8.9 \pm 1.6 \times 10^{-6} \text{ } ^\circ\text{C}^{-1}$ . The expansion of these tuffs is apparently independent of heating rate and orientation and is measurably affected by two mineralogic factors: the presence of cristobalite in some samples, which results in markedly nonlinear expansion between 200° to 300°C; and possible partial alteration of the biotite in biotite-bearing tuffs to expandable clays (vermiculite and/or montmorillonite). Although biotite contents of silicic tuffs are generally small (i.e., less than 3%), alteration of this phase could easily dominate expansion behavior near the boiling point of water.

Expansion behavior of both high- and low-porosity tuffs that contain hydrated silicic glass and/or expandable clays is largely dominated near the boiling point by the dehydration and resultant contraction of these phases. The apparent correlation of porosity and mineralogy in samples

studied here appears to be genetically inherent in tuffs. Because of their structural stability, the most frequently reported zeolites appear not to have a measurable direct effect on the thermal expansion of tuffs.

With the important exception of biotite-free devitrified welded tuffs, variations in fluid pressure affect the expansion behavior of silicic tuffs, since the two major reactions occurring below 200°C involve dehydration of a hydrated phase. The reliability of extrapolation of the results presented to repository depths will depend on: (1) a valid understanding of rate-dependent and fluid-pressure effects upon dehydration behavior of expandable clays and silicic glasses at realistic fluid pressures (these pressures are lower than those normally examined in experimental petrology); and (2) a proper understanding of the effects of both micro- and macrofractures on the thermal expansion of tuff masses, an understanding that can be gained only through in-situ testing. However, based on the results presented here, the thermal expansion uncertainties involved in waste management in silicic tuffs should be minimized by using devitrified welded tuffs free of both appreciable biotite and cristobalite.

## References

1. R. L. Smith, Zones and Zonal Variations in Welded Ash Flows, USGS\*, Prof. Paper 354-F (Washington: Government Printing Office, 1960).
2. P. W. Lipman, R. L. Christiansen, and J. T. O'Connor, A Compositionally Zoned Ash-Flow Sheet in Southern Nevada, USGS, Prof. Paper 524-F (Washington: Government Printing Office, 1966).
3. D. L. Hoover, "Genesis of Zeolites, Nevada Test Site," in E. B. Eckel, ed., Nevada Test Site, Geol. Soc. Am., Mem. 110, 1968, p 275.
4. F. M. Byers, Jr., W. J. Carr, P. P. Orkild, W. D. Quinlivan, and K. A. Sargent, Volcanic Suites and Related Cauldrons of Timber Mountain-Oasis Valley Caldera Complex, Southern Nevada, USGS, Prof. Paper 919 (Washington: Government Printing Office, 1976).
5. R. K. Kirby and T. A. Hahn, Certificate of Analysis, Standard Reference Material 739, Fused Silica, National Bureau of Standards, US Dept. of Commerce (Washington: Government Printing Office, May 12, 1971).
6. R. K. Kirby, National Bureau of Standards, US Dept. of Commerce, Untitled memo to K. Bety, Labtronics, Box 566, 26 Valley Road, Port Washington, NY, October 1, 1971.
7. H. W. Cooper and G. Simmons, "The Effects of Cracks of Thermal Expansion of Rocks," Ear. Plan. Sci. Lett., 36, 1977, p 404.
8. T. F. Wong and W. F. Brace, "Measurements of Thermal Expansion of Rocks at High Pressure (abs.)", EOS 58, 1977, p 1236.
9. N. B. C. Yelamanchili, H&N Nevada Test Site, Memo to A. R. Lappin, Sandia Laboratories, "Physical Properties of Rock Cores From Drill Hole UE25A#1," December 19, 1978.
10. N. B. C. Yelamanchili, H&N Nevada Test Site, Memo to A. R. Lappin, Sandia Laboratories, "Physical Properties of Rock Core Samples From UE25A#1 Drill Hole," April 5, 1979.
11. C. S. Ross and R. L. Smith, Ash-Flow Tuffs, Their Origin, Geologic Relations, and Identification, USGS, Prof. Paper 366 (Washington: Government Printing Office, 1961).
12. R. A. Robie, B. S. Hemingway, and J. R. Fisher, Thermodynamic Properties of Minerals and Related Substances at 298.15 K and 1 Bar (10<sup>5</sup> Pascals) Pressure and at Higher Temperatures, USGS, Bull. 1452, (Washington: Government Printing Office, 1978).

---

\*US Geological Survey

References (cont)

13. R. B. Sosman, The Phases of Silica, (New Brunswick, NJ: Rutgers University Press, 1965).
14. R. L. Smith, "Ash Flows," Geol. Soc. Am. Bull., 71, 1960, p 795.
15. C. S. Ross and R. L. Smith, "Water and Other Volatiles in Volcanic Glasses," Am. Miner., 40, 1955, p 1071.
16. C. W. Burnham and N. F. Davis, "The Role of H<sub>2</sub>O in Silicate Melts I. P-V-T Relations in the System NaAlSi<sub>3</sub>O<sub>8</sub>-H<sub>2</sub>O to 10 Kilobars and 1000°C," Am. Jour. Sci., 270, 1971, p 54.
17. P. W. Lipman, Chemical Comparison of Glassy and Crystalline Volcanic Rocks, USGS Bull. 1201-D (Washington: Government Printing Office, 1965).
18. G. H. Heiken and M. L. Bevier, Petrology of Tuff Units From the J-13 Drill Site, Jackass Flats, Nevada, Los Alamos Scientific Laboratory Informal Report LA-7563-MS, 1979.
19. W. P. Kingery, Introduction to Ceramics (New York: John Wiley and Sons, 1967).
20. C. Colella, R. Aiello, and C. Procelli, "Hydration as an Early State in the Zeolitization of Natural Glass," in L. B. Sand and F. A. Mumpton, eds., Natural Zeolites, Occurrence, Properties, Use (Elmsford, NY: Pergamon Press, 1978).
21. L. V. Benson, Mass Transport in Vitric Tuffs of Rainier Mesa, Nye County, Nevada, US ERDA paper NVO-1253-10, 1976.
22. R. L. Hay and R. A. Sheppard, "Zeolites in Open Hydrologic Systems," F. A. Mumpton, ed., Mineralogy and Geology of Natural Zeolites, Min. Soc. Am., Short Course Notes, 4, 1977, p 93.
23. D. W. Breck, Zeolite Molecular Sieves (New York: John Wiley and Sons, 1974).

APPENDIX

Stratigraphic Positions and Sample Locations of Analyzed Samples

<u>Sample Location and Depth (ft)</u>	<u>Stratigraphic Position</u>
<u>Hole Ue25A#1</u>	
166	
186	Tiva Canyon Member, Paintbrush Tuff
212	
1290	Topopah Springs Member, Paintbrush Tuff
1544	Tuffs of Calico Hills
1555	
1561	
1569	
1861	Prow Pass Member, Crater Flat Tuff
1981	
2365	Bullfrog Member, Crater Flat Tuff
2401	
2427	
2494	
<u>Well J-13</u>	
JA-6	Tiva Canyon Member, Paintbrush Tuff
JA-13	Topopah Springs Member, Paintbrush Tuff
JA-22	"Bedded Tuff," Paintbrush Tuff
JA-29	Bullfrog Member, Crater Flat Tuff
<u>G-Tunnel Complex</u>	
Ev6#3-68	Grouse Canyon Member, Belted Range Tuff
Ev6#3-80	
Ev6#3-115	
Ev6#11-35	Tunnel Bed 4, Local Unit
INST#7-161	Tunnel Bed 5, Local Unit
Ev6#1-181	

DISTRIBUTION:

DOE/TIC-4500-R67 UC-70 (324)

US Department of Energy  
Asst Secretary  
for Defense Programs  
Washington, DC 20545  
Attn: D. C. Sewell (DP-1)

US Department of Energy  
Acting Asst Secretary  
for Energy Technology  
Washington, DC 20545  
Attn: C. Williams (ET-3)

US Department of Energy (9)  
Office of Nucl Waste Management  
Washington, DC 20545  
Attn: S. Meyers (ET-90)  
R. G. Romatowski (ET-90)  
C. A. Heath (ET-960)  
D. L. Vieth (ET-963)  
R. Stein, OW (ET-961)  
C. R. Cooley (ET-961)  
M. W. Frei (ET-963)  
R. H. Campbell (ET-920)  
D. B. LeClaire (ET-920)

US Department of Energy (2)  
Richland Operations Office  
PO Box 550  
Richland, WA 99352  
Attn: F. Standerfer  
D. J. Squires

US Department of Energy  
Albuquerque Operations Office  
PO Box 5400  
Albuquerque, NM 87115  
Attn: T. Schueler, Jr.

US Department of Energy  
San Francisco Operations Office  
1333 Broadway, Wells Fargo Bldg  
Oakland, CA 94612  
Attn: L. Lanni

Rockwell International (2)  
Atomics International Division  
Rockwell Hanford Operations  
Richland, WA 99352  
Attn: R. Deju  
B. Dietz

US Department of Energy (24)  
Nevada Operations Office  
PO Box 14100  
Las Vegas, NV 89114  
Attn: M. E. Gates  
R. W. Taft  
R. W. Newman  
J. B. Cotter  
M. P. Kunich  
H. L. Melancon  
A. J. Roberts  
R. M. Nelson  
D. G. Jackson  
P. J. Mudra  
R. H. Marks, CP-1  
S. R. Elliott  
B. W. Church  
T. H. Blankenship  
R. R. Loux (10)

US Department of Energy (3)  
NTS Support Office  
PO Box 435  
Mercury, NV 89023  
Attn: J. H. Dryden  
F. Huckabee  
L. P. Skousen

DOE Region 9  
Director of External Affairs  
111 Pine Street, 3rd Floor  
San Francisco, CA 94111  
Attn: D. J. Cook

US Department of Energy  
Columbus Program  
Richland Operations Office  
505 King Avenue  
Columbus, OH 43201  
Attn: J. O. Neff

Nuclear Regulatory Commission (2)  
Washington, DC 20555  
Attn: J. C. Malaro, M/S SS674  
R. Boyle, M/S P-522

Holmes & Narver, Inc.  
PO Box 14340  
Las Vegas, NV 89114  
Attn: A. E. Gurrola

DISTRIBUTION: (cont)

Lawrence Livermore Laboratory (7)  
University of California  
PO Box 808  
Livermore, CA 94550  
Attn: L. D. Ramspott, L-204  
A. Holzer, L-209  
L. B. Ballou, L-204  
J. S. Kahn, L-49  
K. Street, L-209  
R. C. Carlson, L-204  
A. B. Miller, L-204

Los Alamos Scientific Laboratory (6)  
University of California  
PO Box 1663  
Los Alamos, NM 87545  
Attn: K. Wolfsberg (2)  
L. S. Germain, M/S 570  
L. Lanham, M/S 755  
B. M. Crowe, M/S 978  
J. R. Smyth, M/S 978

Westinghouse (7)  
PO Box 708  
Mercury, NV 89023  
Attn: D. C. Durrill

Westinghouse - AESD (11)  
PO Box 10864  
Pittsburgh, PA 15236  
Attn: J. B. Wright (6)  
W. R. Morris  
T. E. Cross  
R. J. Bahorich  
C. R. Bolmgren  
W. A. Henninger

University of Arizona  
Nuclear Fuel Cycle Research  
Tucson, AZ 85721  
Attn: J. G. McCray

US Geologic Survey (3)  
National Center  
Reston, VA 22092  
Attn: G. D. DeBuchananne, M/S 410  
P. R. Stevens, M/S 410  
D. B. Stewart, M/S 959

US Geologic Survey (2)  
PO Box 25046  
Federal Center  
Denver, CO 80225  
Attn: G. L. Dixon, M/S 954  
W. S. Twenhofel, M/S 954

Geologic Society of America  
3300 Penrose Place  
Boulder, CO 80302  
Attn: J. C. Frye

University of Kansas  
Kansas Geological Survey  
Lawrence, KS 66044  
Attn: W. W. Hambleton

Battelle (10)  
Office of Nucl Waste Isolation  
505 King Avenue  
Columbus, OH 43201  
Attn: N. E. Carter  
S. Basham  
J. Carr  
ONWI Library (5)  
R. A. Robinson  
W. Carbiner

State of Nevada  
Governor's Office of Planning  
Coordination  
Capitol Complex  
Carson City, NV 89710  
Attn: R. Hill, State  
Planning Coordinator

Fenix & Scisson, Inc.  
PO Box 498  
Mercury, NV 89203  
Attn: F. D. Waltman

State of Nevada  
Capitol Complex  
Carson City, NV 89710  
Attn: N. Clark,  
Dept of Energy

Woodward-Clyde Consultants  
Western Region Library  
No. 3 Embarcadero Center  
San Francisco, CA 94111

DISTRIBUTION: (cont)

Computer Sciences Corp.  
6565 Arlington Blvd  
Falls Church, VA 22046  
Attn: J. Lahoud

John A. Blume Engineers  
Sheraton Palace Hotel  
1340 Jessie Street  
San Francisco, CA 94105  
Attn: P. Yanev

Harvard University (2)  
Dept of Geological Sci &  
Dept of Earth Sciences  
Cambridge, MA 02138  
Attn: R. Siever

Dartmouth College  
Dept of Earth Sciences  
Hanover, NH 03755  
Attn: J. Lyons

Internatl Atomic Energy Agency  
Div of Nucl Power & Reactors  
Karntner Ring 11  
PO Box 590, A-1011  
Vienna, Austria  
Attn: J. P. Colton

Fenix & Scisson, Inc.  
PO Box 15408  
Las Vegas, NV 89114  
Attn: J. A. Cross

Princeton University  
Dept of Civil Engineering  
Princeton, NJ 08540  
Attn: G. Pinder

California Energy Resources  
Conservation & Devel Com  
1111 Howe Avenue  
Sacramento, CA 95825  
Attn: A. Soinski

University of California  
Lawrence Berkeley Laboratory  
Energy & Environment Division  
Berkeley, CA 94270  
Attn: P. Witherspoon

Hanford Eng Development Lab  
PO Box 1970  
Richland, WA 99352  
Attn: D. Cantley

Arthur D. Little, Inc.  
Acorn Park  
Cambridge, MA 02140  
Attn: C. R. Hadlock

Brown University  
Dept of Geological Sciences  
Providence, RI 02912  
Attn: B. Giletti

Texas A&M University  
Center for Tectonophysics  
College Station, TX 77840  
Attn: J. Handin

Law Engineering Testing Co.  
2749 Delk Road, SE  
Marietta, GA 30067  
Attn: B. Woodward

Holmes & Narver, Inc.  
PO Box 1  
Mercury, NV 89023  
Attn: G. E. Christensen

Subcommittee on Energy  
Research & Production  
Room B-374  
Rayburn House Office Bldg  
Washington, DC 20575  
Attn: S. Lanes, Staff Dir.

Dept of Health and Environment  
Bureau of Radiation Control  
Forbes Field  
Topeka, KS 66620  
Attn: G. W. Allen, Director

State of Connecticut  
Energy Research and Policy  
80 Washington Street  
Hartford, CT 06115  
Attn: F. N. Brenneman

Executive Office  
Lansing, MI 48909  
Attn: W. C. Taylor,  
Science Advisor

DISTRIBUTION: (cont)

Dir for Policy and Planning  
325 West Adams St - Room 300  
Springfield, IL 62706  
Attn: A. Liberatore

Nuclear Energy Division  
Nucl Projects Coordinator  
PO Box 14690  
Baton Rouge, LA 70808  
Attn: L. H. Bohlinger

Oregon Dept of Energy  
Labor & Industries Bldg  
Room 111  
Salem, OR 97310  
Attn: D. W. Godard

Radiation Protection Div  
1000 Northeast 10th Street  
PO Box 53551  
Oklahoma City, OK 73152  
Attn: R. L. Craig, Dir

Reynolds Elect & Eng Co., Inc. (6)  
PO Box 14400  
Las Vegas, NV 89114  
Attn: H. D. Cunningham  
W. G. Flangas  
G. W. Adair  
V. M. Milligan  
C. W. Dunnam  
E. J. Beecher

Radiation Health Info Project  
Environmental Policy Inst  
317 Pennsylvania Ave, SE  
Washington, DC 20003  
Attn: E. Walters

State of South Carolina  
Div of Energy Resources  
Edgar A. Brown Bldg  
1205 Pendleton Street  
Columbia, SC 29201  
Attn: L. E. Priester, Jr.

Federal Agency Relations  
1050 17th St, NW  
Washington, DC 20036  
Attn: O. H. Davis, Dir

Environmental Program Supvr  
903 Ninth Street Office Bldg  
Richmand, VA 23219  
Attn: K. J. Buttleman

Energy Administration  
Dept of Natural Resources  
Tawes State Office Bldg  
Annapolis, MD 21401  
Attn: P. Massicot, Actg Dir

State of Ohio Environmental  
Protection Agency  
361 E. Broad St - Box 1049  
Columbus, OH 43216  
Attn: J. F. McAvoy, Dir

State of Connecticut  
House of Representatives  
One Hundred and Sixth District  
24 Rock Ridge Road  
Newtown, CT 06470  
Attn: J. W. Anderson

MO Dept of Natural Resources  
PO Box 176  
Jefferson City, MO 65102  
Attn: T. D. Davis

MS Dept of Natural Resources  
Suite 228, Barefield Complex  
455 North Lamar Street  
Jackson, MS 39201  
Attn: P. T. Bankston

Tennessee Energy Authority  
Suite 708 Capitol Blvd Bldg  
Nashville, TN 37219  
Attn: J. A. Thomas, Assoc Dir

Council Member  
374 South Rock River Drive  
Berea, OH 44017  
Attn: G. A. Brown

Public Law Utilities Group  
One American Pl, Suite 1601  
Baton Rouge, LA 70825  
Attn: D. Falkenheier, Asst Dir

Energy Facility Site Eval Council  
820 East Fifth Ave  
Olympia, WA 98504  
Attn: N. D. Lewis

DISTRIBUTION: (cont)	4413	F. Donath
	4500	E. H. Beckner
University of Texas at Austin	4510	W. D. Weart
University Station, Box X	4512	T. O. Hunter
Austin, TX 78712	4530	R. W. Lynch
Attn: E. G. Wermund	4537	L. D. Tyler (5)
	4537	B. S. Langkopf
Dept for Human Resources	4537	A. R. Lappin (10)
Commonwealth of Kentucky	4537	J. K. Johnstone
Frankfort, KY 40601	4537	D. R. Waymire
Attn: R. M. Fry	4538	R. C. Lincoln
	4541	H. C. Shefelbine
Office of Energy Resources	4732	A. R. Sattler
73 Tremont Street	5500	O. E. Jones
Boston, MA 02108	5510	D. B. Hayes
Attn: L. Morgenstern	5512	D. F. McVey (2)
	5520	T. B. Lane
Dept of Environmental	5521	S. W. Key
Regulation	5521	R. K. Thomas
Twin Towers Office Bldg	5530	W. Herrmann
2600 Blair Stone Road	5541	W. C. Luth
Tallahassee, FL 32301	5623	B. M. Bulmer
Attn: D. S. Kell	8266	E. A. Aas
	3141	T. L. Werner (5)
1417 F. L. McFarling	3151	W. L. Garner (3)
1417 G. F. Rudolfo		For DOE/TIC (Unlimited Release)

